



# **A static and eigenvalue analysis of piezoelectric cantilever energy harvester**

Huan Hu (1437284)

CivE 665: Introduction to Finite Element Analysis

Supervisor: Dr. Samer Adeeb



## **Abstract**

This paper investigated a versatile model for optimizing the performance of a rectangular cantilever beam piezoelectric energy harvester used to convert ambient vibrations into electrical energy. Static analysis was used in an effort to check the validity of structural design. The parameters investigated were: different materials of piezoelectric layer, input force, substrate and piezoelectric layer length, substrate layer width, and substrate layer thickness on output of electrical potential. Findings from a parameter study indicate there is the existence of optimum sample parameters. Performance enhancements were observed using shorter piezoelectric layers as compared to the conventional design, in which the piezoelectric layer and substrate are of equal length. The final geometry of the piezoelectric layer was determined as  $45 \times 3 \times 0.2 \text{ mm}$  and the geometry of the substrate layer is determined as  $50 \times 3 \times 0.7 \text{ mm}$ . Finally, to determine the optimum design configuration for piezoelectric cantilever energy harvesters, an extra mass was added at the end of the beam. The eigenvalue analysis was investigated for the natural frequency. The result shows that the resonant frequency decreases from 413.13 Hz without mass to 200.27 Hz with mass.



## Table of Contents

List of Figures .....	iii
List of Tables .....	v
Background .....	1
Objectives .....	3
Procedure .....	3
Cases and analysis.....	9
Conclusions.....	16
References.....	17



## List of Figures

Figure 1 – The schematic diagram of the energy harvesting .....	1
Figure 2 – The geometry of the piezoelectric beam .....	5
Figure 3 – The elastic setting of the piezoelectric layer .....	5
Figure 4 – The coupling matrix of the piezoelectric layer .....	5
Figure 5 – The dielectric matrix of the piezoelectric layer .....	6
Figure 6 – The assembly model of the piezoelectric beam .....	6
Figure 7 – The restraints of the piezoelectric layer .....	7
Figure 8 – The load and boundary conditions .....	7
Figure 9 – The model after meshing .....	8
Figure 10 – The displacement magnitude after deformed .....	8
Figure 11 – The electrical potential deformed .....	8
Figure 12 – Electrical potential comparisons of different materials .....	9
Figure 13 – Electrical potential comparisons of different thickness .....	10
Figure 14 – Electrical potential comparisons of different width .....	10
Figure 15 – Electrical potential comparisons of different length .....	11
Figure 16 – Electrical potential comparisons of different pressure .....	12
Figure 17 – The electrical potential after deformed .....	12
Figure 18 – The first natural frequency without mass .....	13
Figure 19 – The second natural frequency without mass .....	13
Figure 20 – The third natural frequency without mass .....	14
Figure 21 – The fourth natural frequency without mass .....	14
Figure 22 – The first natural frequency with mass .....	14
Figure 23 – The second natural frequency with mass .....	15
Figure 24 – The third natural frequency with mass .....	15
Figure 25 – The fourth natural frequency with mass .....	16





## List of tables

Table 1 – Previous geometric properties for a piezoelectric beam.....	4
Table 2 – Parameters of different materials .....	9
Table 3 – Parameters of different thickness and electrical potential .....	9
Table 4 – Parameters of different width and electrical potential .....	10
Table 5 – Parameters of different length and electrical potential .....	11
Table 6 – Parameters of different pressure and electrical potential .....	11
Table 7 – The final material parameters of the cantilever .....	12



## BACKGROUND

Vibration energy harvesting has received significant research interests in recent years, owing to both its application potential and technical challenge. The concept has the potential to replace batteries in applications such as wireless sensors, e.g. a type pressure monitoring sensor. The basic mechanisms used for transforming vibrations into electric energy include piezoelectric, electromagnetic, electrostatic, and magnetostrictive transduction. Manufacture can be integrated readily into existing micro electromechanical systems (MEMS) fabrication techniques and the maximum energy storage density exceeds the other transduction mechanisms. A common issue with electromagnetic devices is their low output voltage, requiring the use of a step-up transformer to assist integration with the power electronics. A drawback with electrostatic devices is their inability to function without a separate priming voltage. Piezoelectric devices are not limited by such problems; they have good electrical–mechanical coupling effects. The conventional design for a micro scale piezoelectric energy harvester is based on a cantilever beam configuration, consisting of a substrate layer with attached piezoelectric layers (e.g. lead zirconate titanate (PZT)) and a tip mass to tune the natural frequency of the beam.

The piezoelectrical effect is the coupling of stress and electrical field in a material: an electrical field causes the material to strain, and vice versa. The piezoelectric harvester simply consists of a composite three-layer Euler–Bernoulli beam, with piezoelectric material perfectly bonded to a substrate layer, as shown in figure 1. The working mechanism is that there will be positive piezoelectric effect for piezoelectric material after vibration force. The layer can get the electrical potential finally. The schematic diagram of the energy harvesting is as follows:

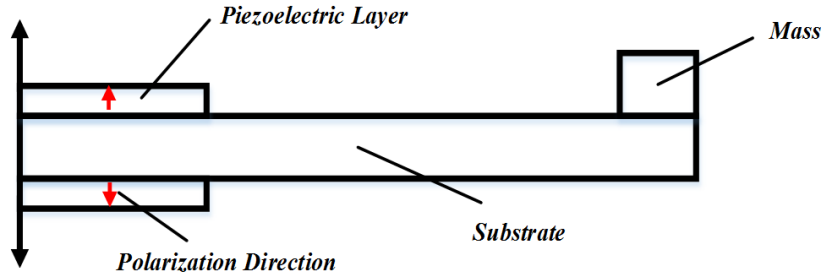


Fig.1.The schematic diagram of the energy harvesting

The linear, coupled matrix differential equations for a piezoelectric energy generator have been previously with respect to the temporal displacements ( $u$ ) and piezoelectric voltage ( $V$ ) as:

$$M\ddot{u} + D\dot{u} + Ku - \Theta V = -M^* a \quad (1)$$

$$\Theta^T \dot{u} + C\dot{V} = I \quad (2)$$

where  $M$ ,  $D$ , and  $K$  are the mass, damping, and stiffness matrices, respectively.  $\Theta$  is the piezoelectric coupling vector,  $C$  is the piezoelectric capacitance,  $I$  is the piezoelectric current,  $M^*$  is the effective mass, and  $a$  is the applied base acceleration. The dots above the variables represent derivatives with respect to time. For simplicity it is assumed that all piezoelectric layers are electrically connected to produce a single output voltage. The

analysis can be directly extended to include multiple electrically disconnected piezoelectric sources. Equation (1) can be rewritten as:

$$M\ddot{u} + D\dot{u} + Ku = -M^*a + F \quad (3)$$

where  $F = \Theta V$  is the vector of applied piezoelectric forces. Equation (3) can be solved using a standard solid mechanics FEM provided that appropriate piezoelectric forces are applied to the structure.

Currently the assumption of linear materials is utilized. The basic constitutive equations for a piezoelectric linear medium are defined in the following:

$$\sigma_i = C_{ik}^E \varepsilon_k - e_{ij}^E E_j \quad (i = 1, 2 \dots 6) \quad (4)$$

$$D_l = e_{lk} \varepsilon_k + \varepsilon_{ij} E_j \quad (l = 1, 2, 3) \quad (5)$$

where  $\sigma_i$  is mechanical stressed;  $\varepsilon_k$  is strain vector;  $E_j$  is the electric field vector;  $C_{ik}^E$  is the short-circuit mechanical stiffness;  $e_{ij}^E$  is electromechanical coupling matrix; and  $\varepsilon_{ij}$  are the dielectric constants.

Here, the piezoelectric is considered as orthotropic material. The function can be expressed as following:

$$\begin{bmatrix} \sigma_{11} \\ \sigma_{22} \\ \sigma_{33} \\ \sigma_{12} \\ \sigma_{13} \\ \sigma_{23} \end{bmatrix} = \begin{bmatrix} c_{11} & c_{12} & c_{13} & 0 & 0 & 0 \\ c_{12} & c_{11} & c_{13} & 0 & 0 & 0 \\ c_{13} & c_{13} & c_{33} & 0 & 0 & 0 \\ 0 & 0 & 0 & c_{66} & 0 & 0 \\ 0 & 0 & 0 & 0 & c_{44} & 0 \\ 0 & 0 & 0 & 0 & 0 & c_{44} \end{bmatrix} \begin{bmatrix} \varepsilon_{11} \\ \varepsilon_{22} \\ \varepsilon_{33} \\ \varepsilon_{23} \\ \varepsilon_{13} \\ \varepsilon_{12} \end{bmatrix} - \begin{bmatrix} 0 & 0 & e_{31} \\ 0 & 0 & e_{31} \\ 0 & 0 & e_{33} \\ 0 & 0 & 0 \\ e_{15} & 0 & 0 \\ 0 & e_{15} & 0 \end{bmatrix} \begin{bmatrix} E_1 \\ E_2 \\ E_3 \end{bmatrix} \quad (6)$$

$$\begin{bmatrix} D_1 \\ D_2 \\ D_3 \end{bmatrix} = \begin{bmatrix} 0 & 0 & 0 & 0 & e_{15} & 0 \\ 0 & 0 & 0 & 0 & 0 & e_{15} \\ e_{31} & e_{31} & e_{33} & 0 & 0 & 0 \end{bmatrix} \begin{bmatrix} \varepsilon_{11} \\ \varepsilon_{22} \\ \varepsilon_{33} \\ \varepsilon_{23} \\ \varepsilon_{13} \\ \varepsilon_{12} \end{bmatrix} + \begin{bmatrix} \lambda_{11} & 0 & 0 \\ 0 & \lambda_{11} & 0 \\ 0 & 0 & \lambda_{33} \end{bmatrix} \begin{bmatrix} E_1 \\ E_2 \\ E_3 \end{bmatrix} \quad (7)$$

FEM software Abaqus can provide the capabilities of piezoelectric analysis and regular piezoelectric elements with the coupling of electric and mechanic. In Abaqus, the constitutive equations are used:

$$\sigma_{ij} = D_{ijkl}^E \varepsilon_{kl} - e_{mkl}^E E_m \quad (8)$$

$$q_i = e_{ijk} \varepsilon_{kl} + D_{ij} E_j \quad (9)$$

The function can be rewritten as:

$$\begin{bmatrix} \sigma_{11} \\ \sigma_{22} \\ \sigma_{33} \\ \sigma_{12} \\ \sigma_{13} \\ \sigma_{23} \end{bmatrix} = \begin{bmatrix} D_{1111} & D_{1122} & D_{1133} & 0 & 0 & 0 \\ D_{2211} & D_{1111} & D_{2233} & 0 & 0 & 0 \\ D_{3311} & D_{3322} & D_{3333} & 0 & 0 & 0 \\ 0 & 0 & 0 & D_{1212} & 0 & 0 \\ 0 & 0 & 0 & 0 & D_{1313} & 0 \\ 0 & 0 & 0 & 0 & 0 & D_{2323} \end{bmatrix} \begin{bmatrix} \varepsilon_{11} \\ \varepsilon_{22} \\ \varepsilon_{33} \\ \varepsilon_{23} \\ \varepsilon_{13} \\ \varepsilon_{12} \end{bmatrix} - \begin{bmatrix} 0 & 0 & e_{311} \\ 0 & 0 & e_{322} \\ 0 & 0 & e_{333} \\ 0 & 0 & 0 \\ e_{133} & 0 & 0 \\ 0 & e_{223} & 0 \end{bmatrix} \begin{bmatrix} E_1 \\ E_2 \\ E_3 \end{bmatrix} \quad (10)$$

$$\begin{bmatrix} q_1 \\ q_2 \\ q_3 \end{bmatrix} = \begin{bmatrix} 0 & 0 & 0 & 0 & e_{113} & 0 \\ 0 & 0 & 0 & 0 & 0 & e_{223} \\ e_{311} & e_{322} & e_{333} & 0 & 0 & 0 \end{bmatrix} \begin{bmatrix} \varepsilon_{11} \\ \varepsilon_{22} \\ \varepsilon_{33} \\ \varepsilon_{23} \\ \varepsilon_{13} \\ \varepsilon_{12} \end{bmatrix} + \begin{bmatrix} D_{11} & 0 & 0 \\ 0 & D_{22} & 0 \\ 0 & 0 & D_{33} \end{bmatrix} \begin{bmatrix} E_1 \\ E_2 \\ E_3 \end{bmatrix} \quad (11)$$

## OBJECTIVE

The main objective is to gain understanding of the influence of geometric parameters on the performance of a piezoelectric cantilever micro scale energy harvester. Thus, the model can get optimum output electrical potential. This purpose is achieved through the development and validation of an analytical model for a cantilever beam piezoelectric energy harvester, and a detailed parameter study. The investigation was mainly concentrated on six different conditions. The six conditions investigated were:

1. Different substrate materials;
2. Different piezoelectric length;
3. Different substrate thickness;
4. Different mechanical forces;
5. Different substrate width;
6. Different applied forces;

Then, the eigenvalue analysis is investigated to get the resonant frequency of the model.

## PROCEDURE

The simple model is made up of two piezoelectric layers and one substrate layer. It is usually called bimorph model. The piezoelectric layer is consisting of the piezoelectric material PZT4, whose dimension is 50mm\*3mm\*0.2mm. While the substrate layer is made of aluminum and has the thickness of 0.6mm. The layers are orthogonal to the axis of polarization and the substrate layer is considered to be completely covered with electrodes. The poling direction is the 3-direction. The electrodes are placed on the faces that are

orthogonal to the 3-axis. The models were drawn using the 3D solid option in ABAQUS. The properties for the materials in the generator are available in Boucher et al. (1981). These properties for the PZT4 are given as

Elasticity Matrix:

$$\begin{bmatrix} D_{1111} & D_{1122} & D_{1133} & 0 & 0 & 0 \\ D_{2211} & D_{1111} & D_{2233} & 0 & 0 & 0 \\ D_{3311} & D_{3322} & D_{3333} & 0 & 0 & 0 \\ 0 & 0 & 0 & D_{1212} & 0 & 0 \\ 0 & 0 & 0 & 0 & D_{1313} & 0 \\ 0 & 0 & 0 & 0 & 0 & D_{2323} \end{bmatrix} = \begin{bmatrix} 132 & 71 & 73 & 0 & 0 & 0 \\ 71 & 132 & 73 & 0 & 0 & 0 \\ 73 & 73 & 115 & 0 & 0 & 0 \\ 0 & 0 & 0 & 30 & 0 & 0 \\ 0 & 0 & 0 & 0 & 26 & 0 \\ 0 & 0 & 0 & 0 & 0 & 26 \end{bmatrix} GPa \quad (12)$$

Piezoelectric Coupling Matrix (Stress Coefficients):

$$\begin{bmatrix} 0 & 0 & e_{311} \\ 0 & 0 & e_{322} \\ 0 & 0 & e_{333} \\ 0 & 0 & 0 \\ e_{133} & 0 & 0 \\ 0 & e_{223} & 0 \end{bmatrix} = \begin{bmatrix} 0 & 0 & -4.1 \\ 0 & 0 & -4.1 \\ 0 & 0 & 14.1 \\ 0 & 0 & 0 \\ 10.5 & 0 & 0 \\ 0 & 10.5 & 0 \end{bmatrix} coulomb / m^2 \quad (13)$$

Dielectric Matrix:

$$\begin{bmatrix} \lambda_{11} & 0 & 0 \\ 0 & \lambda_{11} & 0 \\ 0 & 0 & \lambda_{33} \end{bmatrix} = \begin{bmatrix} 7.12 & 0 & 0 \\ 0 & 7.12 & 0 \\ 0 & 0 & 5.84 \end{bmatrix} 10^{-9} farad / m \quad (14)$$

Table.1. Previous geometric properties for a piezoelectric beam

Structure	Thickness of piezo-layer	Width of piezo-layer	Length of the piezo-layer
Parameters	0.2mm	3mm	50mm
Structure	Thickness of the beam	Width of beam	Length of the beam
Parameters	0.6mm	3mm	50mm

The geometry of the piezoelectric beam is as following:

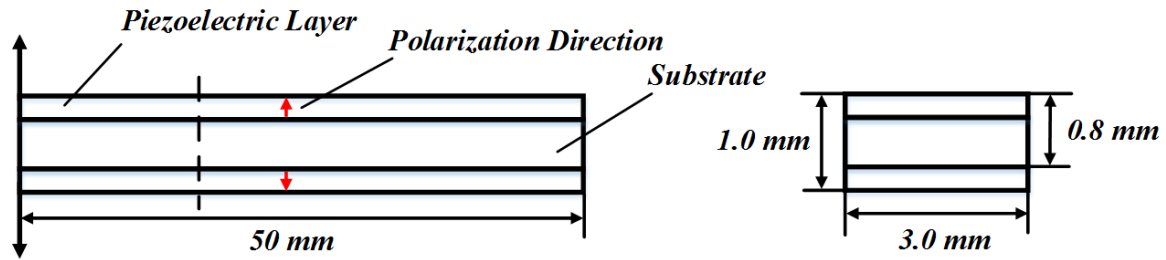


Fig.2.The geometry of the piezoelectric beam

In ABAQUS, the model is set up as following:

- 1) Part: 3D solid extrusion option.
- 2) Property: piezoelectric layer: the material was defined as elastic. The elastic behavior was defined as Orthotropic.

Piezoelectric layer material editor: Mechanical-Elasticity-elastic: type: Orthotropic

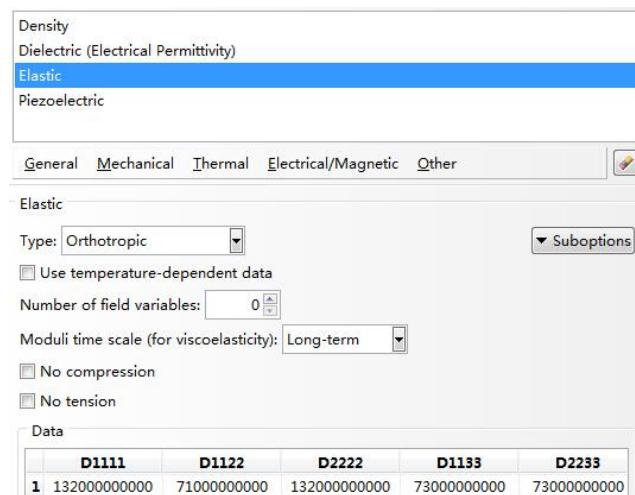


Fig.3.The elastic setting of the piezoelectric layer

Piezoelectric layer material editor: Other-Electrical-Piezoelectric: type: stress

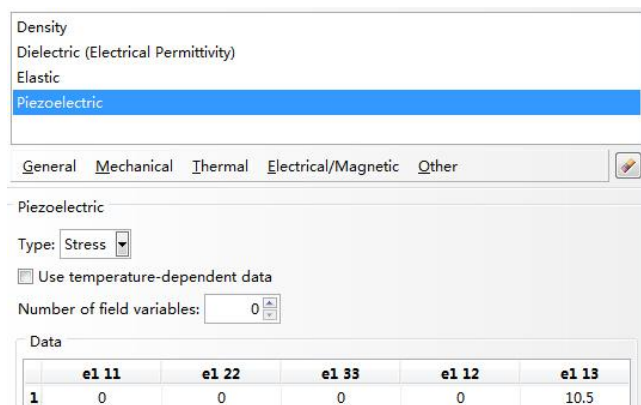


Fig.4.The coupling matrix of the piezoelectric layer

Piezoelectric layer material editor: Other-Electrical-Dielectric: type: orthotropic

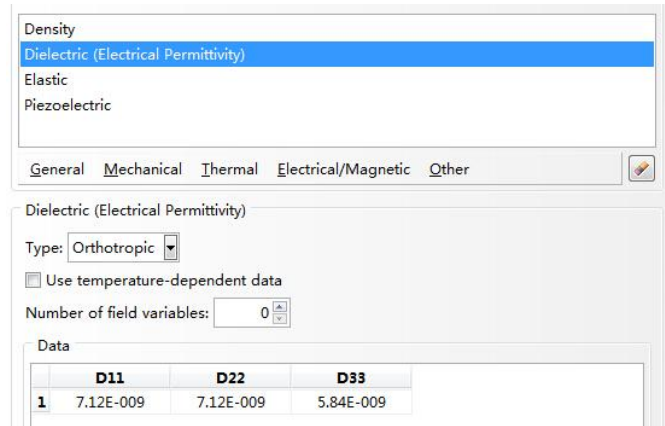


Fig.5.The dielectric matrix of the piezoelectric layer

Substrate layer: the material was defined as elastic. The elastic behavior was defined as isotropic and linear, with Young's modulus of 130 GPa and Poisson's ratio of 0.32.

3) Section: solid-homogeneous; assign section: it is needed to set up local coordinate system for the piezoelectric layer is not isotropic.

4) Assembly:

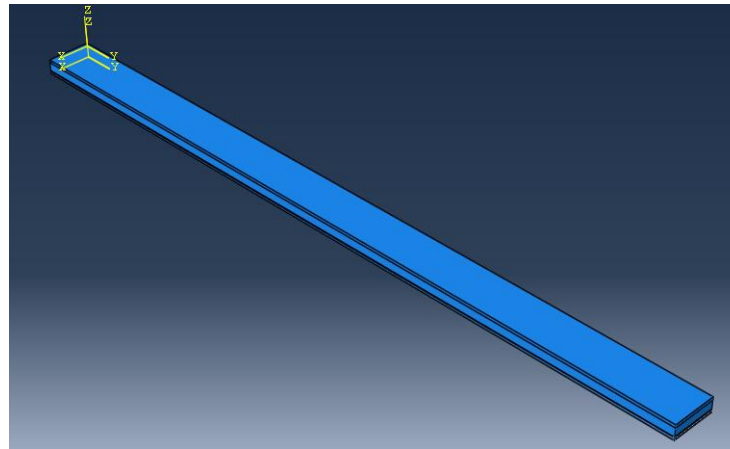


Fig.6.The assembly model of the piezoelectric beam

5) Step: static general analysis. A perfect bond between the substrate and the piezoelectric materials is defined with a surface-based tie constraint, for which the substrate surface is retained as the master surfaces.



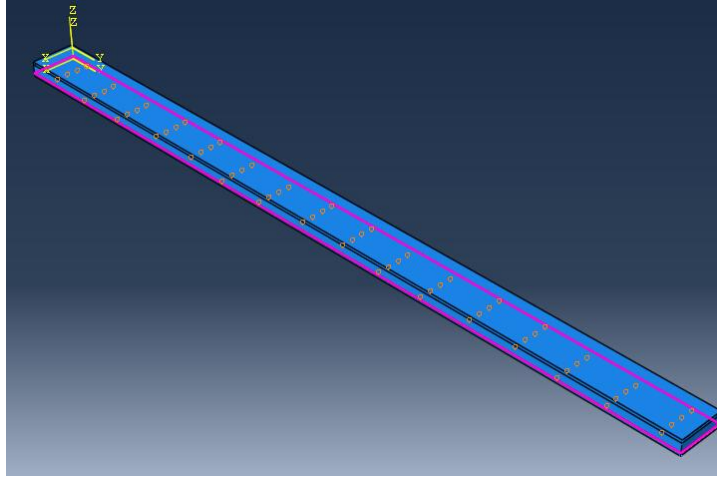


Fig.7.The restraints of the piezoelectric layer

- 6) Load: a distributed pressure force is applied as mechanical load;
- 7) Boundary conditions: the left cantilever is fixed ( $U1 = U2 = U3 = UR1 = UR2 = UR3 = 0$ ), setting the inside of piezoelectric layer of electric potential as zero;

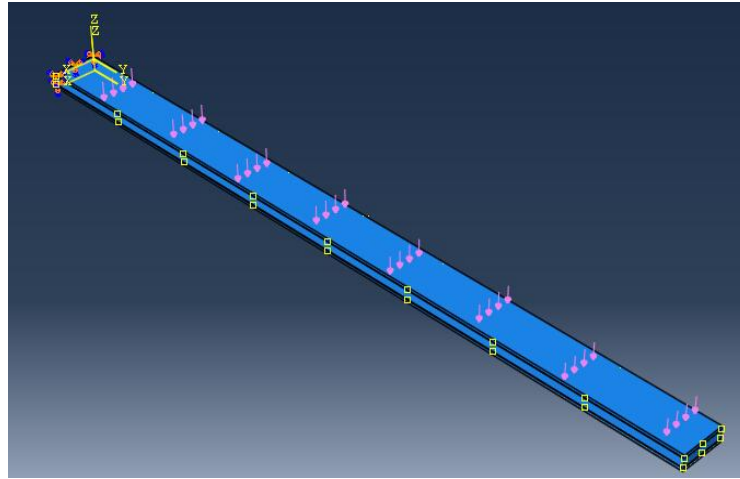


Fig.8.The load and boundary conditions

- 8) Mesh: using 3-noded brick elements (C3D8E), choosing the substrate layer is 3D stress from family, the piezoelectric layer is piezoelectric from family.

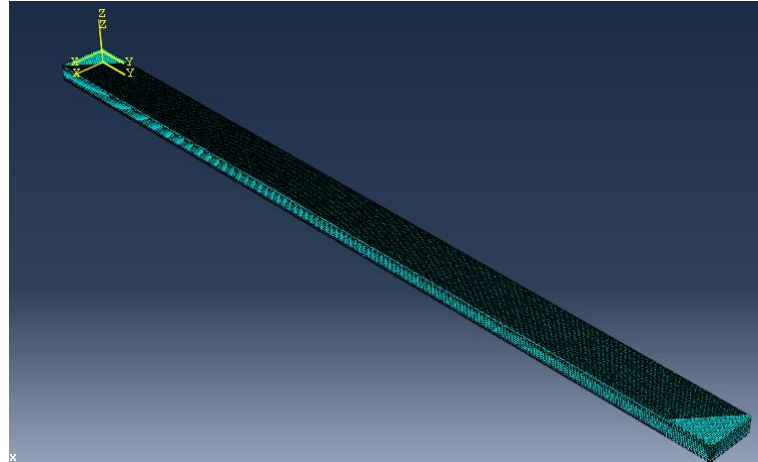


Fig.9.The model after meshing

9) Job:

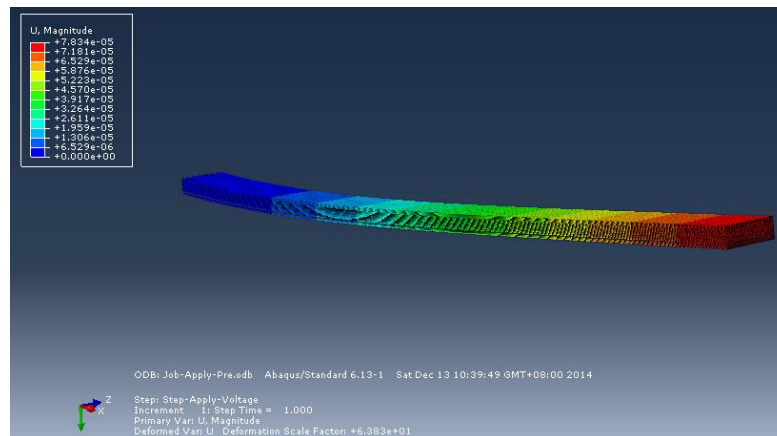


Fig.10.The displacement magnitude deformed

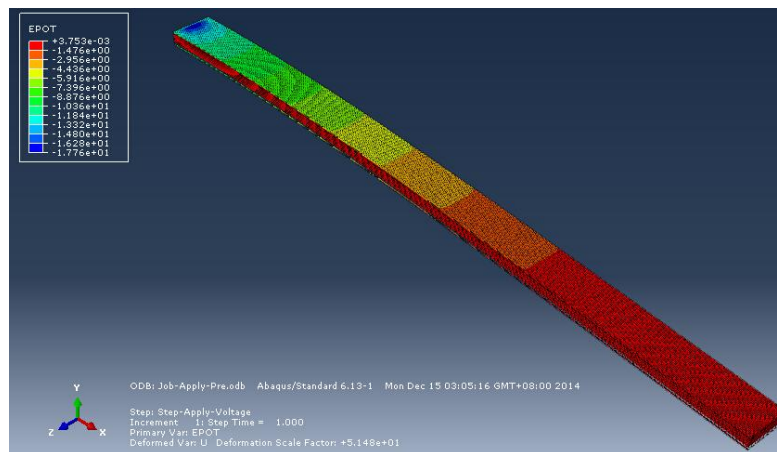


Fig.11.The displacement magnitude after deformation

## CASE STUDY AND ANALYSIS

In this section, detailed discussion will be given about the performance of the output power as a function of these parameters. To get the effect of every single parameter and achieve a fair comparison of results, every related parameter should be taken into account without changing other parameters.

Firstly, different materials of substrate layer are considered.

Table.2. Parameters of different materials

Material	Density( $kg / m^3$ )	Young modules(GPa)	Poisson ratio
Aluminum	2690	70	0.345
Phosphor bronze	8920	106	0.35
Silicon	2328	170	0.278
Steel	7800	197	0.28
Carbon fiber	1760	130	0.32

The comparison of output electrical potential is as following:

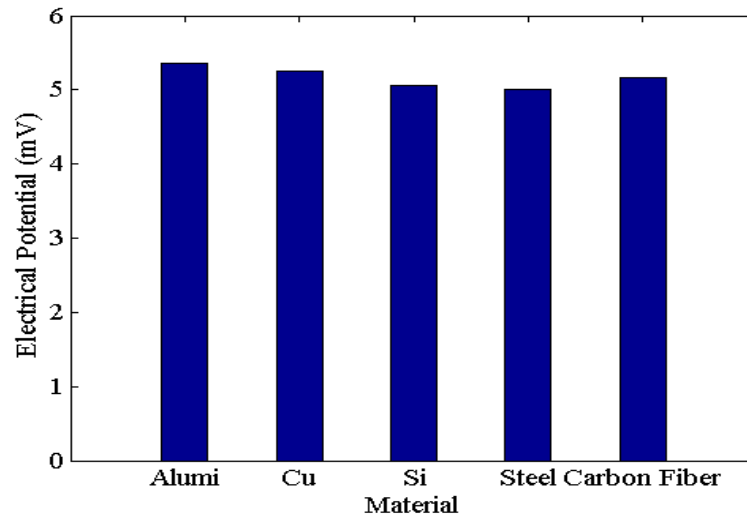


Fig.12.Electrical potential comparisons of different materials

From the figure, we can conclude that the aluminum can get more electrical potential. Thus, we choose aluminum as the substrate material.

Then, the thickness of substrate layer is discussed.

Table.3. Parameters of different thickness and electrical potential

Thickness(mm)	0.1	0.2	0.3	0.4	0.5
Electrical potential(mv)	-0.004895	-0.0051569	-0.00527409	-0.00532924	-0.00535446
Thickness(mm)	0.6	0.7	0.8	0.9	1
Electrical potential(mv)	-0.0053644	-0.00536634	-0.0053641	-0.00535976	-0.00535447

Normalizing the electrical potential of table 3 to positive number, and then plotting with respect to the thickness of the substrate layer, figure 13 is obtained:

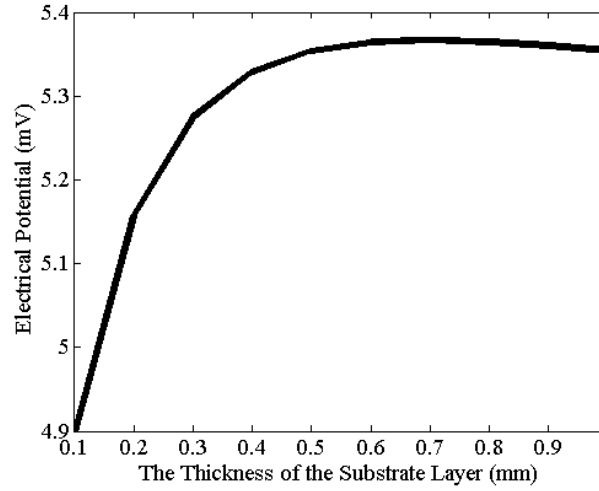


Fig.13.Electrical potential comparisons of different thickness

The influence of width of substrate layer also is discussed to electrical potential.

Table.4. Parameters of different width and electrical potential

Width(mm)	3	6	9	10	12	13	15
Electrical potential(mv)	-0.0053644	-0.00508346	-0.00483931	-0.00365326	-0.00247474	-0.00145284	-0.0006547

The comparison of length to output electrical potential is as following:

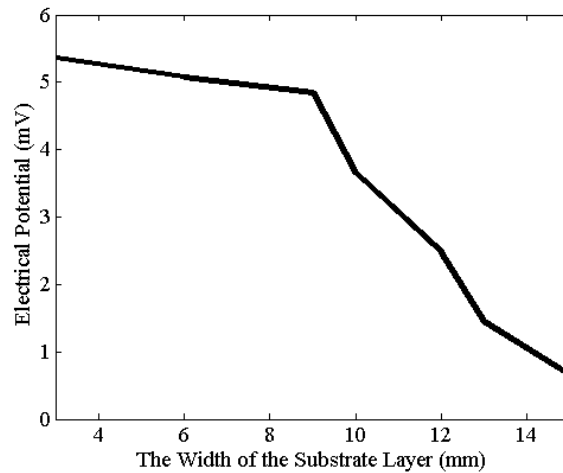


Fig.14.Electrical potential comparisons of different width

The influence of length of substrate layer also is discussed to electrical potential.

Table.5. Parameters of different length and electrical potential

Length(mm)	5	10	15	20	25
Electrical potential(mv)	-0.00543307	-0.00545962	-0.00546018	-0.00546032	-0.00545918
Length(mm)	30	35	40	45	50
Electrical potential(mv)	-0.00546066	-0.00545992	-0.00545987	-0.00546188	-0.0053644

The comparison of length to output electrical potential is as following:

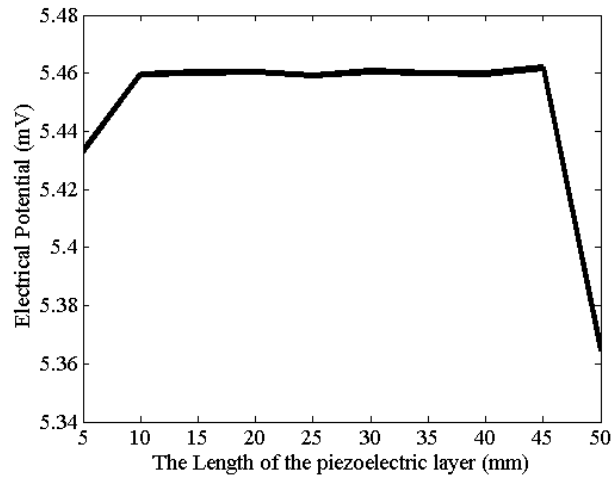


Fig.15.Electrical potential comparisons of different length

The influence of pressure also is discussed to electrical potential.

Table.6. Parameters of different length and electrical potential

Pressure(Pa)	0	200	400	600	800	1000
Electrical potential(mv)	0	-0.00107288	-0.00214576	-0.00321864	-0.00429152	-0.0053644

The comparison of length to output electrical potential is as following:

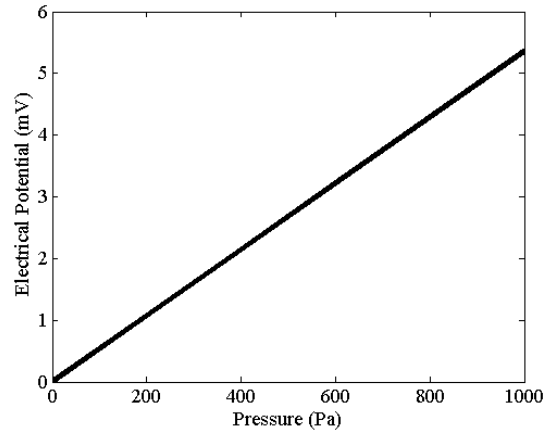


Fig.16.Electrical potential comparisons of different pressure

From the figures above, we can get the conclusion that the output voltage is linear with the input pressure; and with the increase of the substrate width, the output voltage is decreased; with the increase of the piezoelectric length, the output voltage is increased firstly, but it is decreased after 45mm; with increase of the substrate thickness, the output voltage is increased firstly, but it is decreased after 0.7mm. Therefore, we can get the parameters which can make better performance. The final material parameters of the cantilever used for the simulation and design are listed in table 1.

Table.7. The final material parameters of the cantilever

Structure	Thickness of piezo-layer	Width of piezo-layer	Length of the piezo-layer
Parameters	0.2mm	3mm	45mm
Structure	Thickness of the beam	Width of beam	Length of the beam
Parameters	0.7mm	3mm	45mm

The figure is the final geometry for piezoelectric energy harvester.

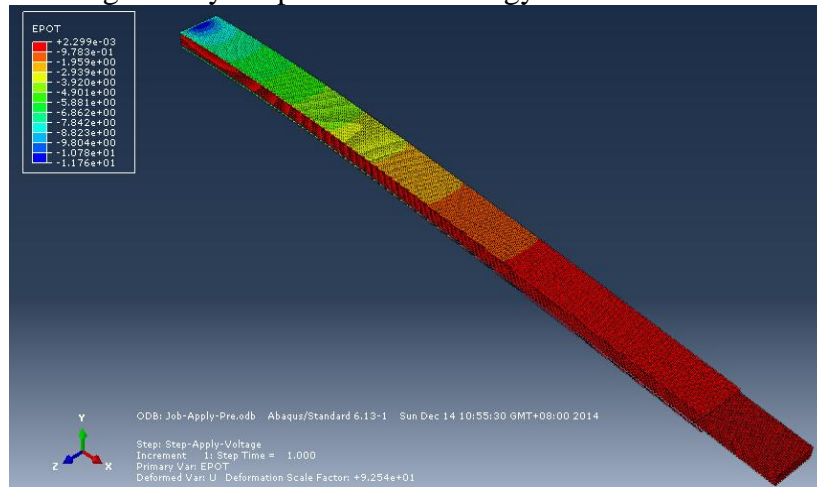


Fig.17.Electrical potential after deformation

## Eigenvalue analysis for piezoelectric energy harvester

In order to produce the maximum deformation of the piezoelectric materials, and consequently to induce maximum electric energy output, the piezoelectric generator operates at the resonance frequency of the vibrational structure. The maximum power is generated at the resonance frequency of the generator. Near the resonance frequency, the mechanical behavior of the structure is well described by a single degree of- freedom (dof) system. After determining the related geometric dimensions, I try to add a mass at the end of to decrease natural frequency. For the vast majority of cases, the ambient vibrations have their energy distributed with significant predominance of low frequency components. The beam is excited at its first bending vibration mode. The frequency is determined at 413.13 Hz as shown in figure 18, which is the resonant frequency without the mass. Figure 19-21 is the results from the second mode to the fourth mode.

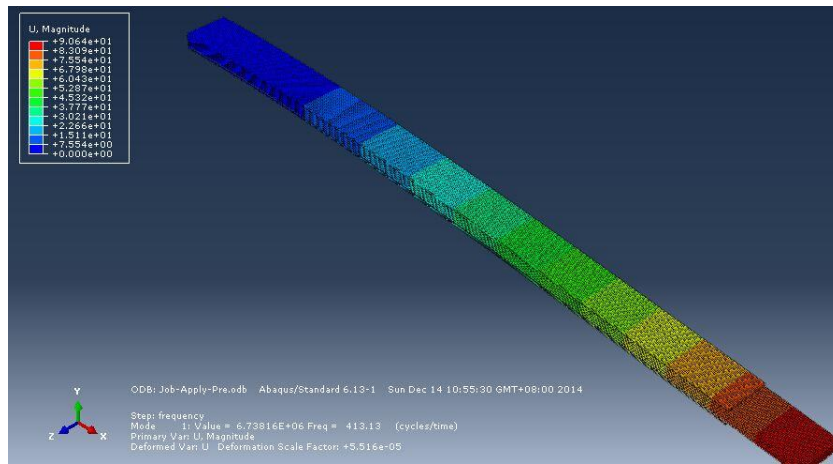


Fig.18.The first natural frequency without mass

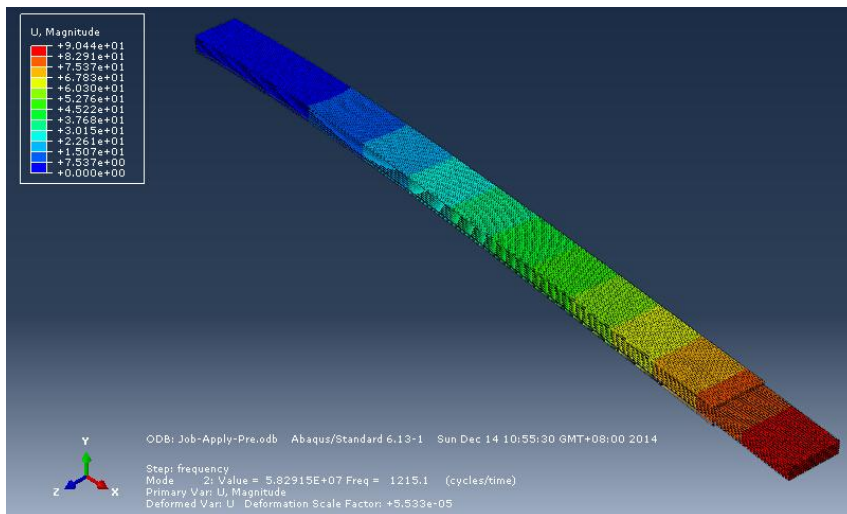


Fig.19.The second natural frequency without mass

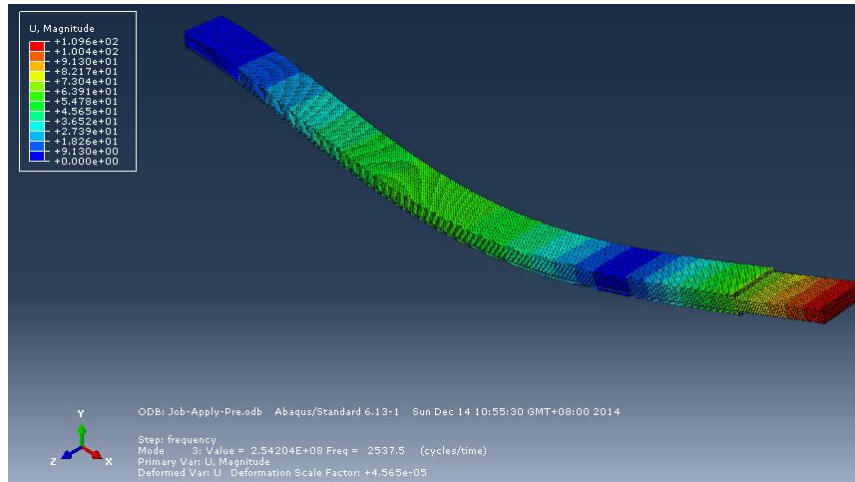


Fig.20.The third natural frequency without mass

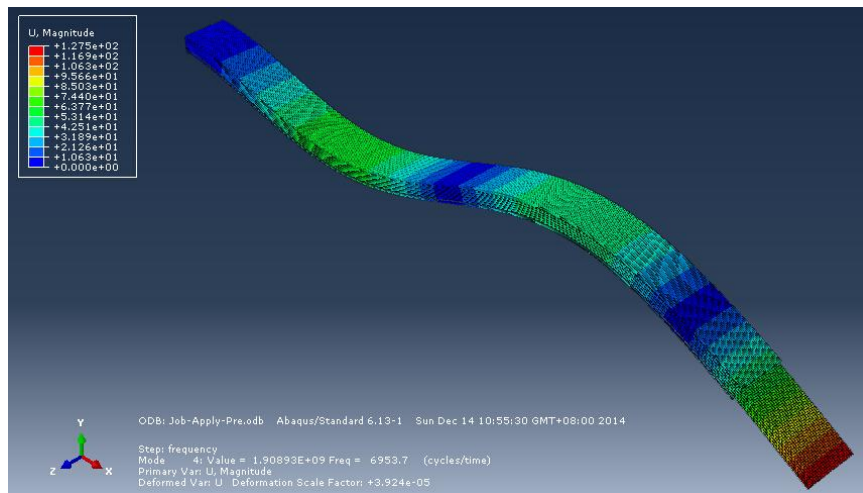


Fig.21.The fourth natural frequency without mass

The frequency is decreased to 200.27 Hz as shown in figure 22 which is the resonant frequency with the mass. Figure 23-25 are the results from the second mode to the fourth mode.

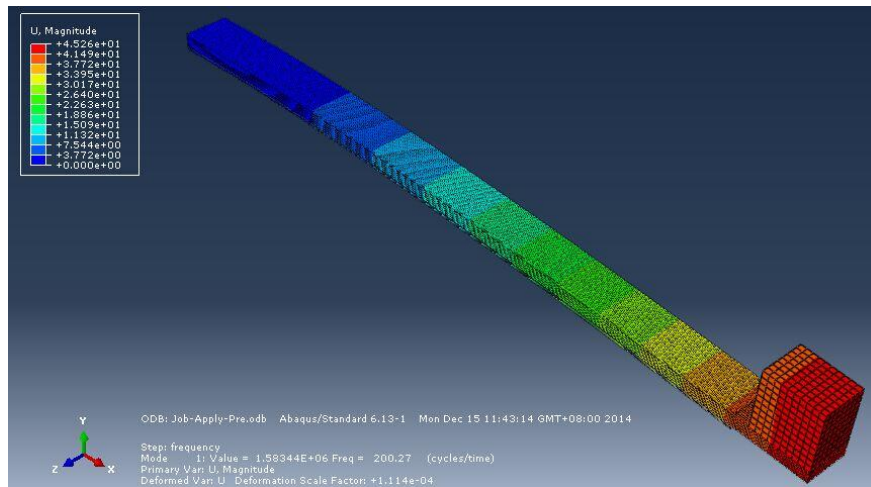


Fig.22.The first natural frequency with mass



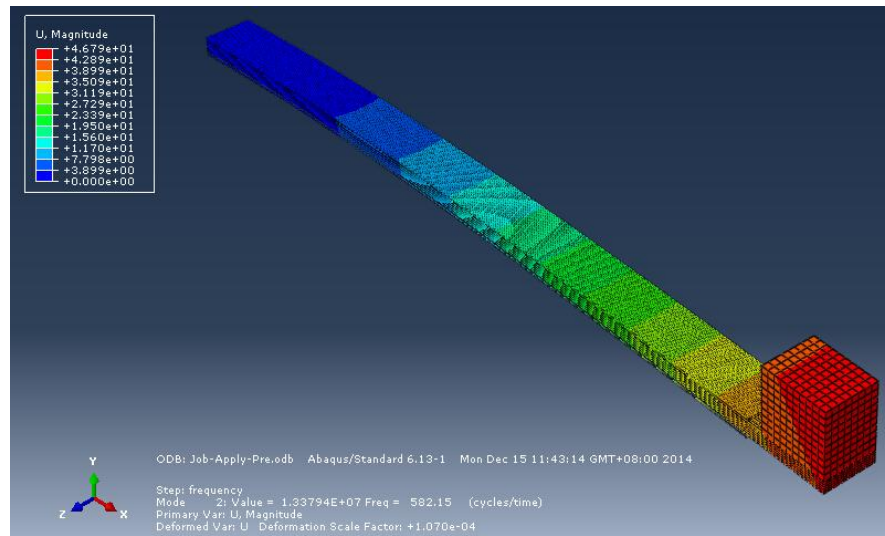


Fig.23.The second natural frequency with mass

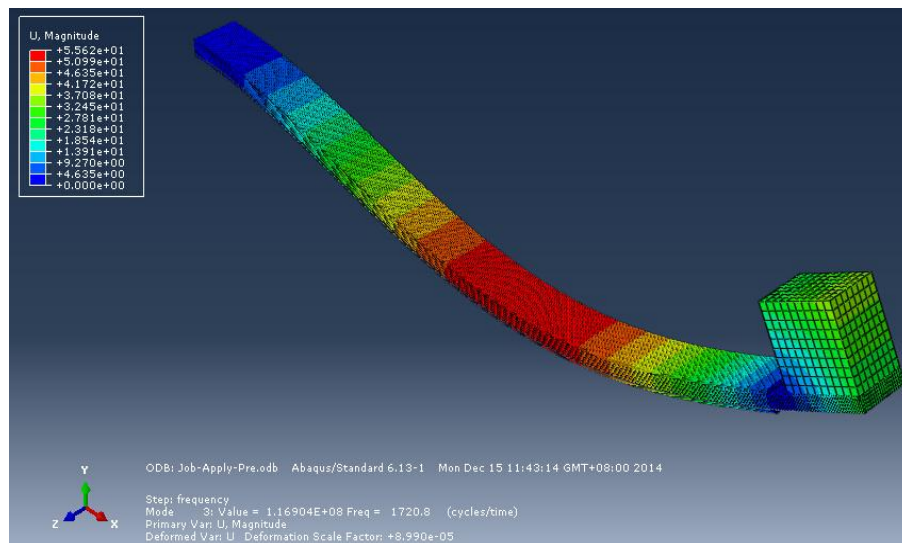


Fig.24.The third natural frequency with mass

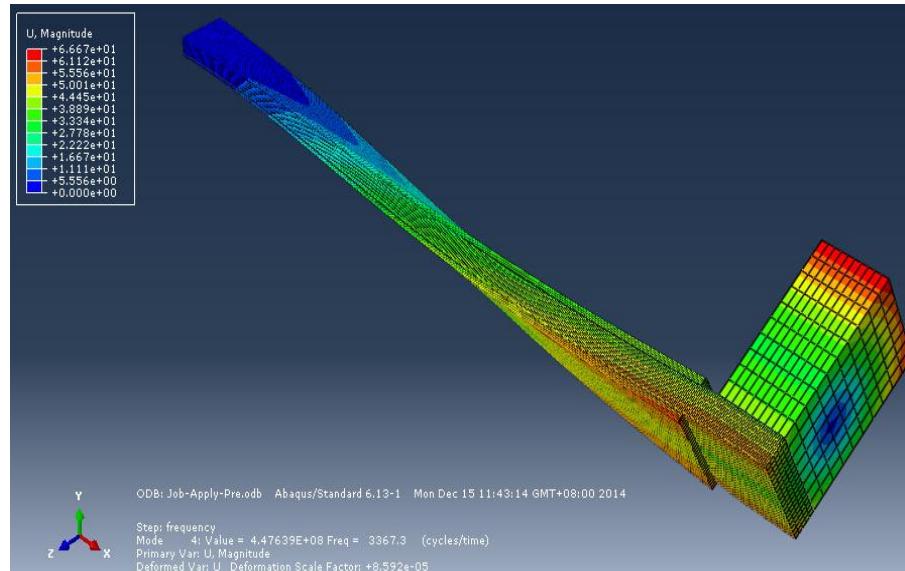


Fig.25.The fourth natural frequency with mass

## CONCLUSION

Firstly, setting the simple model of Euler-Bernoulli beam, it contains two piezoelectric layers and one substrate layer. Because the piezoelectric material contains mechanical-electrical coupling, it can generate the voltage after applying load. So it can be treated as an energy harvester. Then, six related parameters are investigated in ABAQUS to check the validity of the design. After checking the different materials of substrate layer, the aluminum is chosen as the material. At the same time, results show that there is an optimal thickness ratio for the piezoelectric bimorph cantilever harvester; the substrate layer is 3.5 times than piezoelectric layer. The results show that there is an optimal width ratio for the piezoelectric bimorph cantilever harvester; the substrate layer is same as piezoelectric layer. Finally, the optimal parameters are confirmed, which is  $50 \times 3 \times 0.7\text{mm}$  for substrate layer and  $45 \times 3 \times 0.2\text{mm}$  for piezoelectric layer.

Finally, to obtain more energy, reducing the resonant frequency is needed. So the eigenvalue analysis is made to extract natural frequency for four modes. The result shows that the first mode is 413.13 Hz for the optimal geometry. After adding a mass at the end of the beam, the frequency reduced to 200.27 Hz for the first mode.

## REFERENCES

- [1] Anton, S. R., & Sodano, H. a. (2007). A review of power harvesting using piezoelectric materials (2003–2006). *Smart Materials and Structures*, 16(3), R1–R21.
- [2] F. Cottone, H. Vocca, and L. Gammaitoni (2009). Nonlinear Energy Harvesting. *PHYSICAL REVIEW LETTERS*, 080601-080604.
- [3] R Patel, S McWilliam and A A Popov. A geometric parameter study of piezoelectric coverage on a rectangular cantilever energy harvester (2011). *Smart Mater. Struct.* 20 085004 (12pp).
- [4] F Lu, HP Lee, and S P Lim. Modeling and analysis of micro piezoelectric power generators for micro electromechanical systems applications(2004). *Smart Mater. Struct.* 13 57–63.
- [5] Niell G. Elvin, and Alex A. Elvin. A Coupled Finite Element-Circuit Simulation Model for Analyzing Piezoelectric Energy Generator (2009). *Journal of intelligent material systems and structures*, Vol. 20, 587-595.
- [6] Kan J W, Tang K H, Wang S Y, et al. Modeling and simulation of piezoelectric cantilever generators(2008). *Opt. Precision Eng.* 16(1), 71-75.
- [7] U.V. Wagner. Piezo-beam systems subjected to weak electric field: experiments and modelling of non-linearities (2002), *J. Sound Vibr* -256(5), 861—872.
- [8] Shashank Priya, Daniel J. Inman. Energy harvesting technologies(2009).
- [9] <http://50.16.176.52/thesis/search/?query=extract+frequency&submit.x=65&submit.y=7&group=bk&CDB=v6.13>.
- [10] Y.B. Jeon, R. Sood, J.H. Jeong, MEMS power generator with transverse mode thin film PZT (2005), *Sensors and Actuators*, A122, 16-2.
- [11] G.W. Taylor, J.R. Burns, A Small Subsurface Ocean/River Power Generator[2001], *IEEE Journal of Oceanic Engineering*, 26(4), 539-547.